

# Relativistic field-theory spin and momentum in water waves

K. Y. Bliokh<sup>1</sup>, H. Punzmann<sup>2</sup>, H. Xia<sup>2</sup>, F. Nori<sup>1,3</sup>, and M. Shats<sup>2</sup>

<sup>1</sup>*Theoretical Quantum Physics Laboratory, RIKEN Cluster for Pioneering Research,  
Wako-shi, Saitama 351-0198, Japan*

<sup>2</sup>*Research School of Physics, The Australian National University,  
Canberra, ACT 2601, Australia*

<sup>3</sup>*Physics Department, University of Michigan, Ann Arbor, Michigan 48109-1040, USA*

**Spin is a fundamental yet somewhat enigmatic intrinsic angular-momentum property of quantum particles or fields [1–3], which appears within relativistic quantum mechanics or field theory [4,5]. The spin density in wave fields is described by the theoretical Belinfante-Rosenfeld construction based on the difference between the canonical and kinetic energy-momentum tensors [5–7]. These quantities have an abstract mathematical character and are usually considered as non-observable *per se*. Here we demonstrate, both theoretically and experimentally, that the Belinfante-Rosenfeld construction naturally arises in purely classical gravity (surface-water) waves [8]. There, the canonical momentum is associated with the generalized Stokes-drift phenomenon [9], while the spin is generated by subwavelength circular motion of water particles in inhomogeneous wave fields. Thus, we reveal the canonical spin and momentum in water waves and directly observe these fundamental relativistic field-theory properties as microscopic mechanical properties of particles in a classical wave system. Our findings shed light onto the nature of spin and momentum in wave fields and offer a new platform for studies of previously hidden aspects of quantum-relativistic physics.**

Spin angular momentum was first introduced to physics empirically in 1925 by Uhlenbeck and Goudsmit [1]. This allowed them to explain peculiarities of the emission spectra of solids and electron interactions with magnetic fields by a quantum “self-rotation” of electrons. Later, this new property was derived rigorously within the Dirac equation providing the quantum relativistic theory of electrons [4]. Nowadays, spin is essential for the majority of quantum and condensed-matter systems [3], ranging from basic properties of elementary particles and chemical elements, via widely used memory and tomography devices, to the advanced fields of spintronics [10,11] and quantum computing [12–14].

As early as in 1909, Poynting described the intrinsic angular momentum of circularly-polarized light (i.e., an electromagnetic wave with rotating electric and magnetic field vectors) [15]. This property was later observed via optical torque on matter, and it was associated with the spin of photons (i.e., relativistic massless quanta of light) [4,16–19]. Thus, the spin angular momentum naturally appears in classical electromagnetic fields [18–21] where it plays an important role in optical manipulation, light-matter interactions, information transfer, etc. [18,19,22–24]. Recently, it was shown that inhomogeneous acoustic (sound-wave) fields also possess a nonzero spin angular momentum density, which can be associated with the microscopic circular motion of the acoustic-medium particles [25–29].

Theoretically, various kinds of quantum and classical waves are described within the corresponding field theories [4,5]. There, one of the main objects characterizing dynamical properties of the field is the energy-momentum tensor, which includes the field energy and momentum densities. In 1940, Belinfante and Rosenfeld found a fundamental structure in this tensor, which explains the appearance of spin angular momentum and relates it to the momentum properties of the field [5–7]. They showed that there are canonical (non-symmetric, derived from the Noether theorem) and kinetic (symmetrized) versions of the energy-momentum tensor, which contain the corresponding canonical and kinetic momentum densities,  $\mathbf{P}$  and  $\mathbf{\Pi}$ , related as

$$\mathbf{\Pi} = \mathbf{P} + \frac{1}{2} \nabla \times \mathbf{S}, \quad (1)$$

where  $\mathbf{S}$  is the spin angular momentum density. This fundamental relation describes the appearance of spin in both quantum particles and classical (electromagnetic and acoustic) wave fields [2,5,19,21,23,26,29–31].

Despite such progress and thorough exploration of spin in various fields, this fundamental physical entity remains somewhat enigmatic and hidden by quantum-mechanical and relativistic field theory concepts [1–5]. Indeed, the “self-rotation” of the electron described by the Dirac spinors is far from an intuitively clear picture. Furthermore, the canonical momentum and spin densities in the field-theory relation (1) are usually regarded as unobservable *per se* [5–7], and only their integral values matter. In classical fields, rotating angular momentum properties underlying spin are more obvious, but rotating electric and magnetic fields in circularly-polarized light [15–24] or rotating medium particles in inhomogeneous sound waves [26–29] are never observed directly.

The purpose of this work is twofold. First, we will describe and observe the presence of spin in another kind of wave field, namely, in *gravity water waves* [8]. We will show that the water-wave spin is described precisely by the same field-theory relation (1) involving the canonical and kinetic momenta. Second, we will provide the direct observation of the motion of water particles underlying the spin and canonical-momentum densities (1). In doing so, the rotational motion of particles corresponds to the spin density  $\mathbf{S}$ , whereas the translational motion due to the generalized Stokes drift [9] corresponds to the canonical momentum density  $\mathbf{P}$ . To the best of our knowledge, this is the first direct observation of the microscopic origin of the spin angular momentum and canonical momentum in wave fields.

To begin with, [Table I](#) lists the main dynamical quantities involved in Eq. (1) for monochromatic electromagnetic waves in free space [19–21,23,29–31] and sound waves in a fluid or gas [26–29]. For all kinds of monochromatic waves, we consider complex space-dependent field amplitudes  $\mathbf{F}(\mathbf{r})$ , so that real time-dependent fields are  $\text{Re}[\mathbf{F}(\mathbf{r})e^{-i\omega t}]$ , where  $\omega$  is the wave frequency. In this manner, electromagnetic waves are described by the complex electric and magnetic fields,  $\mathbf{E}(\mathbf{r})$  and  $\mathbf{H}(\mathbf{r})$ , while acoustic waves are described by the complex velocity field  $\mathbf{v}(\mathbf{r})$  and scalar pressure field  $p(\mathbf{r})$ . In both electromagnetic and acoustic cases, the canonical momentum density  $\mathbf{P}$  is determined by the form  $\text{Im}[\mathbf{F}^* \cdot (\nabla)\mathbf{F}]$  entirely similar to the probability current in quantum mechanics, i.e., the local “expectation value” of the canonical quantum-mechanical momentum operator  $-i\nabla$  [30,31]. In turn, the spin angular momentum density  $\mathbf{S}$  is determined by the form  $\text{Im}(\mathbf{F}^* \times \mathbf{F})$  which points into the direction normal to the polarization ellipse of the field  $\mathbf{F}$  and is proportional to its ellipticity [18,19,32].

Notably, both electromagnetic and acoustic canonical momentum and spin densities in monochromatic fields are measurable via radiation forces and torques on small absorbing particles [19,26,28,31]. Note also that spatial integrals of the spin densities for localized circularly-polarized paraxial electromagnetic waves and sound wavefields are in agreement with the quantum-mechanical spin values of  $\hbar$  per photon [18,19] and 0 per phonon [27,29]. Substituting the canonical momentum and spin densities into Eq. (1) and using the equations of motion for the wave fields (i.e., Maxwell and acoustic wave equations), one obtains the kinetic momentum density  $\mathbf{\Pi}$ . It is given by the well-known Poynting vector for electromagnetic waves [33] and its acoustic analogue for sound waves [8].

Importantly, the acoustic spin and canonical momentum densities can be immediately associated with the mechanical properties of microscopic particles of the medium. Generally, such particles experience a combination of rotational and translational motion in the sound-wave field. First, the microscopic periodic motion of the medium particles is generically *elliptical* and

corresponds to the polarization of the vector velocity field  $\mathbf{v}$ . The oscillating velocity field  $\mathbf{v}e^{-i\omega t}$  corresponds to the displacement field  $\mathbf{a}e^{-i\omega t} = i\omega^{-1}\mathbf{v}e^{-i\omega t}$ , which yields the time-averaged mechanical angular momentum density  $(\rho/2)\text{Re}(\mathbf{a}^* \times \mathbf{v})$  (where  $\rho$  is the mass density of the medium) [26,29], precisely equivalent to the spin density  $\mathbf{S}$  in Table I. Second, the medium particles in a sound-wave field can experience the slow *Stokes drift* [9], a phenomenon known in hydrodynamics for surface water waves and related to the difference between the Eulerian and Lagrangian velocities of the particles. The momentum density associated with the Stokes drift can be written as (Supplementary Information)  $(\rho/2)\text{Re}[(\mathbf{a}^* \cdot \nabla)\mathbf{v}]$ , which for sound waves with  $\nabla \times \mathbf{v} = \mathbf{0}$  yields the canonical momentum density in Table I. To the best of our knowledge, this feature has not been emphasized before, and the oscillatory and drift motions in inhomogeneous sound waves have never been observed directly due to the very small displacements  $\mathbf{a}$  in typical sound wave fields.

	Electromagnetism	Acoustics	Water waves
Wave fields	electric $\mathbf{E}$ , magnetic $\mathbf{H}$	velocity $\mathbf{v}$ , pressure $p$	In-plane velocity $\mathbf{V}$ , vertical velocity $W$
Kinetic momentum density $\Pi$	$\frac{1}{2c^2}\text{Re}(\mathbf{E}^* \times \mathbf{H})$	$\frac{1}{2c_s^2}\text{Re}(p^* \mathbf{v})$	$\frac{\rho k}{\omega}\text{Im}(W^* \mathbf{V})$
Canonical momentum density $\mathbf{P}$	$\frac{1}{4\omega}\text{Im}[\varepsilon \mathbf{E}^* \cdot (\nabla)\mathbf{E} + \mu \mathbf{H}^* \cdot (\nabla)\mathbf{H}]$	$\frac{\rho}{2\omega}\text{Im}[\mathbf{v}^* \cdot (\nabla)\mathbf{v}]$	$\frac{\rho}{2\omega}\text{Im}[\mathbf{V}^* \cdot (\nabla_2)\mathbf{V} + W^* \nabla_2 W]$
Spin AM density $\mathbf{S}$	$\frac{1}{4\omega}\text{Im}(\varepsilon \mathbf{E}^* \times \mathbf{E} + \mu \mathbf{H}^* \times \mathbf{H})$	$\frac{\rho}{2\omega}\text{Im}(\mathbf{v}^* \times \mathbf{v})$	$\frac{\rho}{2\omega}\text{Im}(\mathbf{V}^* \times \mathbf{V})$

**Table I. The momentum and spin properties of electromagnetic, acoustic, and deep-water gravity monochromatic wavefields.** Here  $c$  is the speed of light,  $c_s$  is the speed of sound,  $\varepsilon$  and  $\mu$  are the permittivity and permeability of the electromagnetic medium, and  $\rho$  is the mass density of the acoustic medium.

We now consider a wave system which has never been associated with spin: surface water (gravity) waves [8]. Deep-water gravity waves are characterized by the dispersion  $\omega^2 = kg$  ( $g$  is the gravitational acceleration,  $k$  is the wave number), and all wave fields decay exponentially from the unperturbed water surface  $z = 0$  deep into the water  $z < 0$  as  $\propto \exp(kz)$  [8]. Thus, in contrast to the 3D electromagnetism and acoustics, this system is quasi-2D. Therefore, we separate the 3D velocity of the water particles in the gravity-wave field,  $\mathbf{v}$ , into the in-plane 2D vector  $\mathbf{V} = (v_x, v_y)$  and the normal component  $W = v_z$ . We will focus on the 2D motion of water particles in the  $(x, y)$  plane, but will also take into account all physical properties related to the vertical  $z$ -motion. The 2D gradient (momentum) operator is  $\nabla_2 = (\partial_x, \partial_y)$ , while the vector product (spin) operator “ $\times$ ” acting in the plane can only produce a  $z$ -directed vertical spin.

Since the motion of water particles in the oscillating 2D velocity field  $\mathbf{V}e^{-i\omega t}$  is entirely similar to the motion of medium particles in the oscillating sound-wave field  $\mathbf{v}e^{-i\omega t}$ , the  $z$ -directed angular momentum density can be written akin to the acoustic spin density:  $(\rho/2\omega)\text{Im}(\mathbf{V}^* \times \mathbf{V})$ . This yields the *spin density*  $\mathbf{S}$  for gravity waves associated with polarization of the vector field  $\mathbf{V}$ , see [Table I](#). This spin appears in inhomogeneous (e.g., interference) water-wave fields, because of the circular (or, generically, elliptical) motion of water particles in the  $(x, y)$  plane.

Next, the water particles experience the Stokes drift [9]. So far, this phenomenon has been known for the circular motion of water particles in the plane orthogonal to the water surface, i.e., involving the vertical velocity component  $W$ . For inhomogeneous wave fields with a nonzero spin  $\mathbf{S}$ , the particles can also exhibit elliptical orbits in the projection onto the water-surface plane. This produces the Stokes drift described by the in-plane velocity  $\mathbf{V}$ . Calculating the total Stokes drift in an arbitrary monochromatic gravity-wave field, we obtain that its velocity is given by (Supplementary Information)  $\mathbf{u} = (2\omega)^{-1} \text{Im}[\mathbf{V}^* \cdot (\nabla_2)\mathbf{V} + W^* \nabla_2 W]$ . Multiplying this Stokes drift velocity by the mass density  $\rho$ , we obtain the *canonical momentum density*  $\mathbf{P}$  for gravity waves, see [Table I](#). Importantly, the Stokes drift, i.e., the canonical momentum, produces the *mass transport* in water waves, such as, e.g., the driftwood along the ocean coasts [34].

Now, substituting the above canonical momentum and spin densities into the Belinfante-Rosenfeld relation (1), we derive the kinetic momentum density  $\mathbf{\Pi}$  for surface water waves, see [Table I](#). Remarkably, its form becomes equivalent to the water-wave momentum density derived by Peskin [35] (Supplementary Information), which can be associated with the *energy flux* density. This completes the description of the momentum and spin densities in deep-water gravity waves. We emphasize that, on the one hand, our description is based on the microscopic mechanical properties of water particles, and, on the other hand, it satisfies the fundamental relativistic field-theory description of spin and momentum densities in wave fields.

We are now in a position to show explicit examples of surface water waves with nonzero spin and momentum. The first example is a simple interference of two plane waves with equal frequencies and orthogonal wavevectors  $\mathbf{k}_1 \perp \mathbf{k}_2$ . The spin and momentum in two-wave interference has been previously considered for optical and sound waves [26,29,36]. Choosing the  $y$ -axis to be directed along  $\mathbf{k}_1 + \mathbf{k}_2$ , we find that the spin and canonical-momentum densities are (Supplementary Information):  $\mathbf{S} \propto -\bar{\mathbf{z}} \sin \tilde{x}$  and  $\mathbf{P} \propto \bar{\mathbf{y}}(2 + \cos \tilde{x})$ , where  $\tilde{x} = \sqrt{2}kx$  and the overbar indicates the unit vectors of the corresponding axes. The distributions of these densities, together with the numerically calculated microscopic water-particle trajectories, are shown in [Fig. 1b](#). One can clearly see that the canonical momentum density corresponds to the Stokes drift of the particles (which everywhere occurs in the  $y$ -direction), whereas the spin density corresponds to the microscopic elliptical motion of particles (which has alternating  $x$ -dependent directions).

We have performed an experiment demonstrating the above motion of water particles and, thereby, the presence of canonical momentum and spin in the two-wave interference, [Fig. 1](#). The experimental setup is shown in [Fig. 1a](#) (see Supplementary Information for details). Interfering gravity waves were generated in a wave tank of size  $1.0 \times 0.6 \text{ m}^2$  and depth  $h = 0.1 \text{ m}$  by two orthogonal paddles driven by two synchronized computer-controlled shakers. We worked with the wave frequencies  $\omega/2\pi \in (3, 9) \text{ Hz}$  which corresponds to the wavelengths  $2\pi/k \in (0.03, 0.17) \text{ m}$  satisfying the deep-water condition  $\tanh(kh) \approx 1$ . Fluid motion at the water surface was visualized using buoyant tracer particles (Polyamid,  $50 \mu\text{m}$ ) illuminated by a LED panel placed underneath the transparent wave tank. A video camera on top was used to capture the motion of the tracer particles.

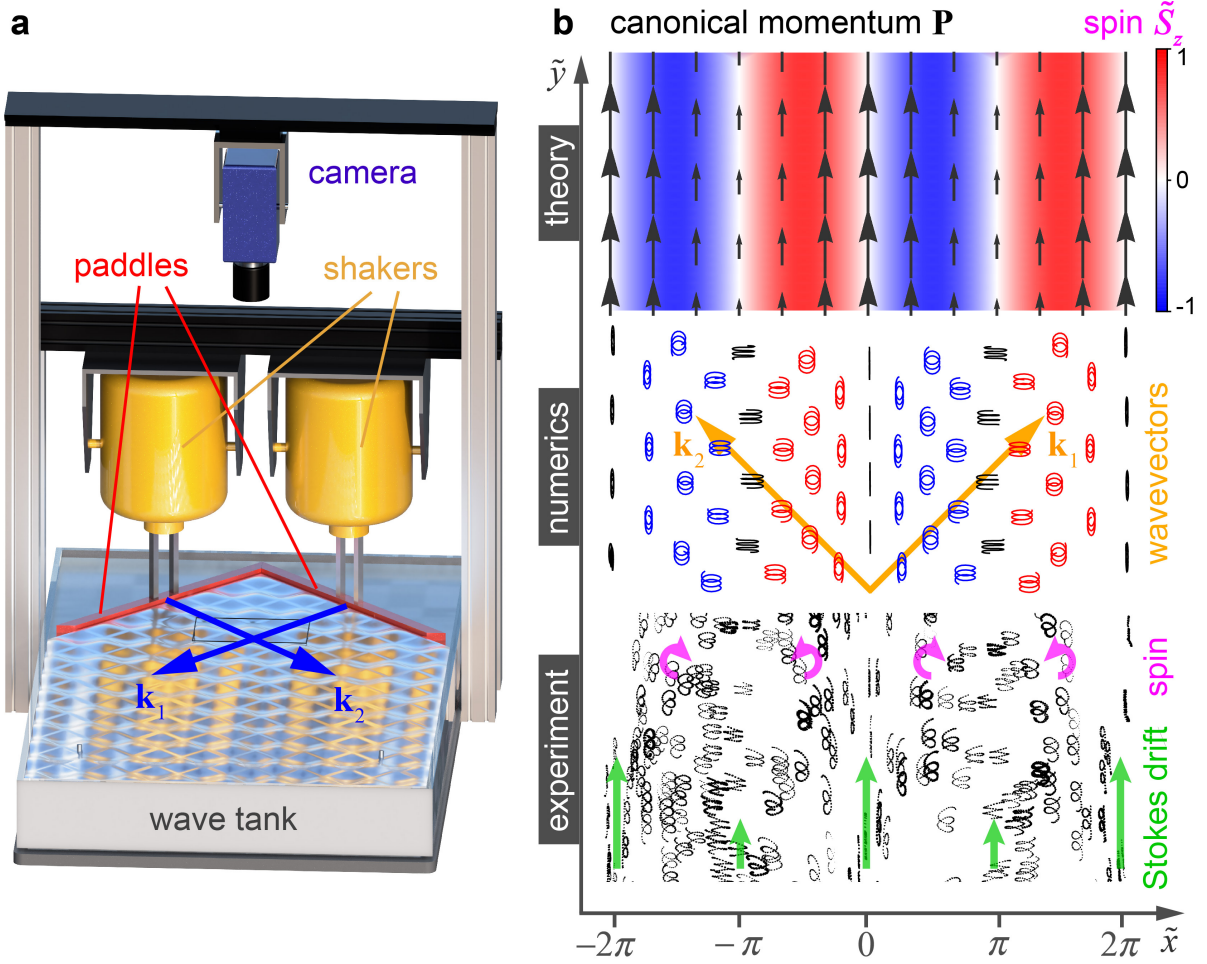


**Figure 1. The canonical momentum and spin densities in interfering surface water waves.** **a**, Schematic of the experimental setup for the observation of the particle motion in interfering gravity waves. **b**, Spin and momentum properties of two interfering gravity waves with equal frequencies, amplitudes, and orthogonal wavevectors  $\mathbf{k}_1$  and  $\mathbf{k}_2$ . The theoretical plot shows the distributions of the canonical momentum density  $\mathbf{P}$  and spin density  $\mathbf{S}$ , [Table I](#). Numerical and experimental plots depict trajectories of microscopic particles for three wave periods  $6\pi/\omega$ . The Stokes drift of the particles and their circular motion correspond to the canonical momentum and spin, respectively. Parameters are:  $\tilde{x} = \sqrt{2}kx$ ,  $\tilde{y} = \sqrt{2}ky$ , and  $\omega/2\pi = 6$  Hz.

In [Fig. 1b](#), one can see that the experimentally measured trajectories are very similar to the numerically-calculated ones. To show that these experimental observations are in quantitative agreement with the theoretical spin and momentum densities, we measure the spatial and frequency dependences of the drift velocities and rotational radii of the particles. First, the canonical momentum density should behave as  $P_y \propto k/\omega \propto \omega$  because the gradient operator scales as  $\propto k$ . Obviously, the particle drift velocity  $u$  should obey the same frequency dependence. Second, the spin density is inversely proportional to the frequency:  $S_z \propto \omega^{-1}$ . As we have discussed, the spin can be associated with the mechanical angular momentum of water particles. At the points of maximum absolute value of the spin,  $\tilde{x} = \pm\pi/2$ , the water particles follow near-circular orbits of radius  $a$  (see [Fig. 1b](#)), and their angular momentum is  $\propto a^2\omega$ . Therefore, this radius should depend on the frequency as  $a \propto \omega^{-1}$ . [Figure 2](#) shows the experimentally measured dependences  $u(\omega)$  and  $a(\omega)$  for water particles. These dependences are in excellent agreement with the above theoretical

predictions and the  $x$ -dependence  $\propto (2 + \cos \tilde{x})$  of the canonical momentum. The only discrepancy is that the drift velocity is offset by a constant value such that  $u(0) \neq 0$ . This is due to the presence of small return flows in the finite-size wave tank (Supplementary Information).

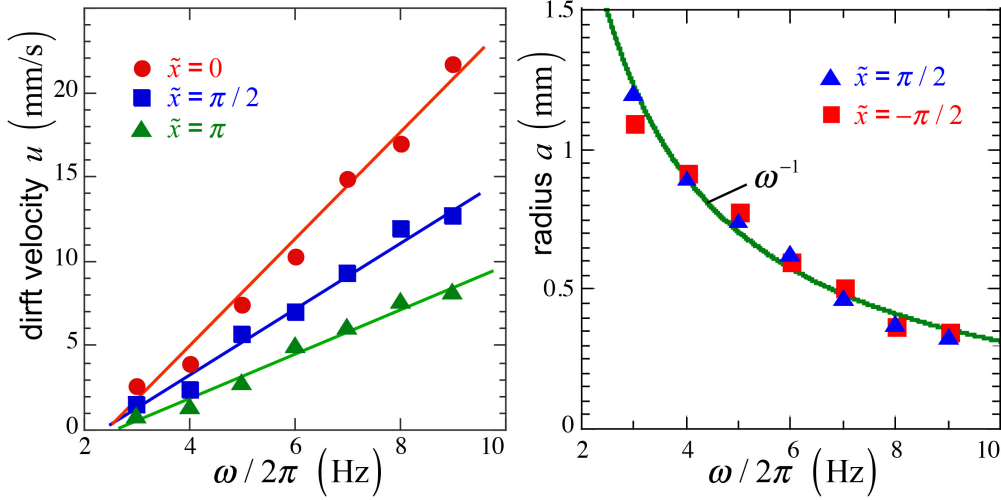


**Figure 2. Frequency dependencies of the Stokes drift and the microscopic orbits in interfering gravity waves from Fig. 1.** The experimentally measured Stokes drift velocity grows linearly with the wave frequency and depends on the position  $\tilde{x} = \sqrt{2}kx$ . The radii of the circular motion of water particles at the maxima of the spin density are inversely proportional to the wave frequency. These dependences are in perfect agreement with theoretical predictions based on the canonical momentum and spin densities.

As another example, we consider an interference of two orthogonal standing water waves with equal amplitudes and frequencies, which is equivalent to four propagating waves. In this case, the spin density forms a periodic chessboard-like structure (see Supplementary Information and Fig. 3):  $\mathbf{S} \propto \bar{\mathbf{z}} \sin \varphi \cos \tilde{x} \cos \tilde{y}$ , where  $\tilde{x} = kx$ ,  $\tilde{y} = ky$ , and  $\varphi$  is the phase between the two orthogonal standing waves. In turn, the canonical momentum density forms vortex-like flows around the maxima and minima of the spin density [37]:  $\mathbf{P} \propto \sin \varphi (\bar{\mathbf{y}} \sin \tilde{x} \cos \tilde{y} - \bar{\mathbf{x}} \cos \tilde{x} \sin \tilde{y})$  (see Supplementary Information and Fig. 3). Figure 3 shows the numerically calculated and experimentally measured trajectories of microscopic particles in the interference of two orthogonal standing waves with  $\varphi = \pi/2$  (the spinless case  $\varphi = 0$  is shown in Supplementary Information). One can see that particles follow large wavelength-scale vortex-like orbits due to the Stokes drift associated with the momentum  $\mathbf{P}$ . Simultaneously, the particles experience microscopic elliptical motion around their current positions, which produces the local angular momentum associated with the spin  $\mathbf{S}$ . We emphasize that the two orbital motions here have different scales and qualitatively different nature. Indeed, the radius of the microscopic spin-related circular motion is proportional to the *amplitude* of the wave and can be made as small as needed, while the radius of the macroscopic vortex-like motion is fixed by the *wavelength*.

To conclude, we have revealed the fundamental spin and momentum properties in surface-water (gravity) waves. Surprisingly, these quantities are precisely described by the relativistic field-theory construction by Belinfante-Rosenfeld [5–7], which underpins the spin and momentum of quantum and classical particles and fields [19,21,23,26,29–31]. We have shown that the canonical momentum density in acoustic and water waves can be directly associated with the mass transfer due to the generalized Stokes drift [9], while the spin density originates from the mechanical angular momentum of the medium particles following microscopic elliptical trajectories. Most

importantly, we have provided the direct observation of these drift and rotational dynamics of water particles in inhomogeneous gravity-wave fields. This can be regarded as the first direct observation of the microscopic origin of the canonical spin and momentum in structured wavefields.

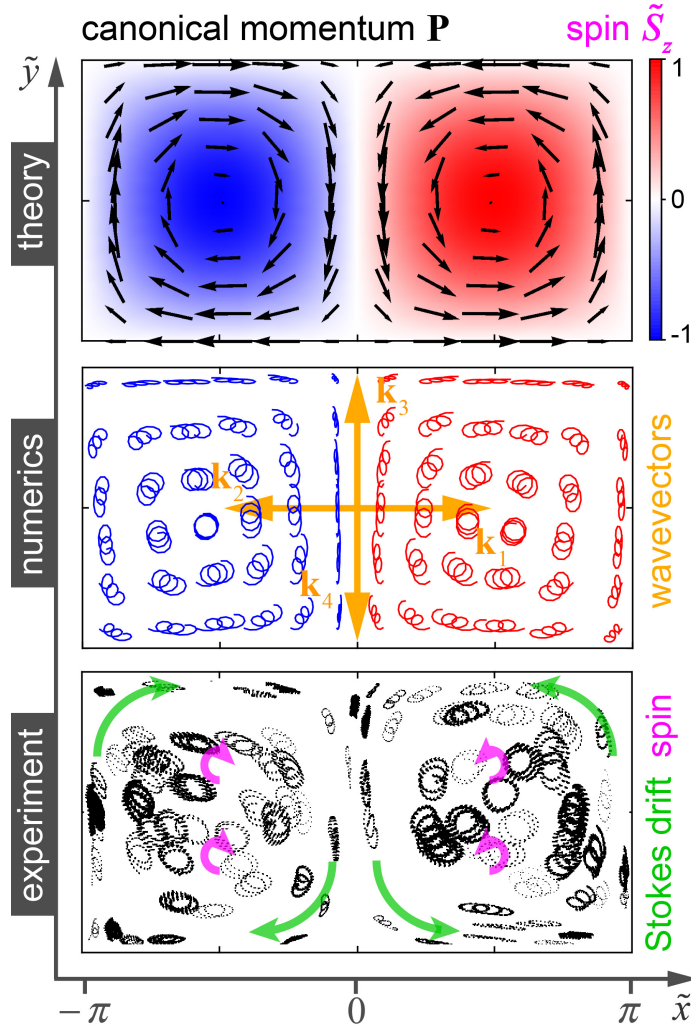


**Figure 3. Canonical momentum and spin densities in the interference of standing gravity waves.** Same as in Fig. 1 but for two interfering orthogonal standing waves with equal frequencies and amplitudes (i.e., equivalently, four propagating plane waves with the wavevectors  $\mathbf{k}_{1,2,3,4}$ ). Parameters are:  $\tilde{x} = kx$ ,  $\tilde{y} = ky$ ,  $\omega / 2\pi = 5.3$  Hz, and  $\varphi = \pi / 2$ .

Our results can have a multifold interdisciplinary impact. First, they illuminate fundamental field-theory relations, which so far have been considered as abstract mathematical formulas underlying observable physical phenomena on a higher level. Second, our findings shed light onto the nature of water-wave and acoustic momentum, which caused longstanding discussions and controversies [35,38]. The presence of nonzero spin density explains the presence of two (canonical and kinetic) momenta, as well as the direct observability of one of these. Third, using the dynamical spin and momentum concepts, one can produce structured water-wave fields for desired manipulation of small particles, including transport and rotation, akin to optical manipulations [18,19,28,39]. Finally, our work offers a new platform for future studies of spin-related field-theory phenomena using readily accessible classical waves.

## References

1. G. E. Uhlenbeck and S. Goudsmit, “Spinning Electrons and the Structure of Spectra”, *Nature* **117**, 264–265 (1926).
2. H. C. Ohanian, “What is spin?”, *Am. J. Phys.* **54**, 500–505 (1986).
3. “Spin”, *Nature Milestones* S5–S20 (2008).
4. V. B. Berestetskii, E. M. Lifshitz, and L. P. Pitaevskii, *Quantum Electrodynamics* (Pergamon, Oxford, 1982).
5. D. E. Soper, *Classical Field Theory* (Wiley, New York, 1976).
6. F. J. Belinfante, “On the current and the density of the electric charge, the energy, the linear momentum and the angular momentum of arbitrary fields”, *Physica* **7**, 449–474 (1940).
7. L. Rosenfeld, “On the energy-momentum tensor”, *Memoirs Acad. Roy. de Belgique* **18**, 1–30 (1940).
8. L.D. Landau and E.M. Lifshitz, *Fluid Mechanics* (Butterworth-Heinemann, Oxford, 1987).
9. G. G. Stokes, “On the theory of oscillatory waves”, *Trans. Cambridge Phil. Soc.* **8**, 441–455 (1847); Reprinted in: G. G. Stokes, *Mathematical and Physical Papers*, Vol. 1, 197–229 (Cambridge University Press, Cambridge, 2009).
10. S. A. Wolf, D. D. Awschalom, R. A. Buhrman, J. M. Daughton, S. von Molnar, M. L. Roukes, A. Y. Chtchelkanova, and D. M. Treger, “Spintronics: A Spin-Based Electronics Vision for the Future”, *Science* **294**, 1488–1495 (2001).
11. I. Zutic, J. Fabian, and S. Das Sarma, “Spintronics: Fundamentals and applications”, *Rev. Mod. Phys.* **76**, 323–410 (2004).
12. I. Buluta, S. Ashhab, and F. Nori, “Natural and artificial atoms for quantum computation”, *Rep. Prog. Phys.* **74**, 104401 (2011).
13. J. J. Pla, K. Y. Tan, J. P. Dehollain, W. H. Lim, J. J. L. Morton, D. N. Jamieson, A. S. Dzurak, and A. Morello, “A single-atom electron spin qubit in silicon”, *Nature* **489**, 541–545 (2012).
14. L. M. K. Vandersypen, H. Bluhm, J. S. Clarke, A. S. Dzurak, R. Ishihara, A. Morello, D. J. Reilly, L. R. Schreiber, and M. Veldhorst, “Interfacing spin qubits in quantum dots and donors – hot, dense, and coherent”, *npj Quantum Inf.* **3**, 34 (2017).
15. J. H. Poynting, “The wave-motion of a revolving shaft, and a suggestion as to the angular momentum in a beam of circularly-polarized light”, *Proc. R. Soc. Lond. Ser. A* **82**, 560–567 (1909).
16. R. A. Beth, “Mechanical detection and measurement of the angular momentum of light”, *Phys. Rev.* **50**, 115–125 (1936).
17. N. B. Simpson, K. Dholakia, L. Allen, and M. J. Padgett, “Mechanical equivalence of spin and orbital angular momentum of light: an optical spanner”, *Opt. Lett.* **22**, 52–54 (1997).
18. D. L. Andrews and M. Babiker, Eds., *The Angular Momentum of Light* (Cambridge University Press, Cambridge, 2013).
19. K. Y. Bliokh and F. Nori, “Transverse and longitudinal angular momenta of light”, *Phys. Rep.* **592**, 1–38 (2015).
20. R. P. Cameron, S. M. Barnett, and A. M. Yao, “Optical helicity, optical spin and related quantities in electromagnetic theory”, *New J. Phys.* **14**, 053050 (2012).
21. K. Y. Bliokh, A. Y. Bekshaev, and F. Nori, “Dual electromagnetism: helicity, spin, momentum and angular momentum”, *New J. Phys.* **15**, 033026 (2013).
22. K. Y. Bliokh, F. J. Rodríguez-Fortuño, F. Nori, and A. V. Zayats, “Spin-orbit interactions of light”, *Nat. Photon.* **9**, 796–808 (2015).
23. A. Aiello, P. Banzer, M. Neugebauer, and G. Leuchs, “From transverse angular momentum to photonic wheels”, *Nat. Photon.* **9**, 789–795 (2015).
24. P. Lodahl, S. Mahmoodian, S. Stobbe, A. Rauschenbeutel, P. Schneeweiss, J. Volz, H. Pichler, and P. Zoller, “Chiral quantum optics”, *Nature* **541**, 473–480 (2017).
25. Y. Long, J. Ren, and H. Chen, “Intrinsic spin of elastic waves”, *Proc. Natl Acad. Sci. USA* **115**, 9951–9955 (2018).

26. C. Shi, R. Zhao, Y. Long, S. Yang, Y. Wang, H. Chen, J. Ren, and X. Zhang, “Observation of acoustic spin”, *Natl. Sci. Rev.* **6**, 707–712 (2019).
27. K. Y. Bliokh and F. Nori, “Spin and orbital angular momenta of acoustic beams”, *Phys. Rev. B* **99**, 174310 (2019).
28. I. D. Toftul, K. Y. Bliokh, M. I. Petrov, and F. Nori, “Acoustic Radiation Force and Torque on Small Particles as Measures of the Canonical Momentum and Spin Densities”, *Phys. Rev. Lett.* **123**, 183901 (2019).
29. L. Burns, K. Y. Bliokh, F. Nori, and J. Dressel, “Acoustic versus electromagnetic field theory: scalar, vector, spinor representations and the emergence of acoustic spin”, *New J. Phys.* **22**, 053050 (2020).
30. M. V. Berry, “Optical currents”, *J. Opt. A: Pure Appl. Opt.* **11**, 094001 (2009).
31. K. Y. Bliokh, A. Y. Bekshaev, and F. Nori, “Extraordinary momentum and spin in evanescent waves”, *Nat. Commun.* **5**, 3300 (2014).
32. M. V. Berry and M. R. Dennis, “Polarization singularities in isotropic random vector waves,” *Proc. R. Soc. Lond. A* **457**, 141–155 (2001).
33. M. Born and E. Wolf, *Principles of Optics* (Cambridge University Press, Cambridge, 1999)
34. M. Kubota, “A mechanism for the accumulation of floating marine debris north of Hawaii”, *J. Phys. Oceanogr.* **24**, 1059–1064 (1994).
35. C. S. Peskin, “Wave momentum”, The Silver Dialogues, New York University (2010); [https://www.math.nyu.edu/faculty/peskin/papers/wave\\_momentum.pdf](https://www.math.nyu.edu/faculty/peskin/papers/wave_momentum.pdf).
36. A. Y. Bekshaev, K. Y. Bliokh, and F. Nori, “Transverse Spin and Momentum in Two-Wave Interference”, *Phys. Rev. X* **5**, 011039 (2015).
37. N. Francois, H. Xia, H. Punzmann, P. W. Fontana, and M. Shats, “ Wave-based liquid-interface metamaterials,” *Nat. Commun.* **8**, 14325 (2017).
38. M. E. McIntyre, “On the ‘wave momentum’ myth”, *J. Fluid Mech.* **106**, 331–347 (1981).
39. D. G. Grier, “A revolution in optical manipulation”, *Nature* **424**, 810–816 (2003).

**Acknowledgements:** This work was partially supported by the Australian Research Council (via the Discovery Grant No. DP190100406 and Linkage Grant No. LP160100477), NTT Research, Army Research Office (ARO) (Grant No. W911NF-18-1-0358), Japan Science and Technology Agency (JST) (via the CREST Grant No. JPMJCR1676), Japan Society for the Promotion of Science (JSPS) (via the KAKENHI Grant No. JP20H00134 and the grant JSPS-RFBR Grant No. JPJSBP120194828), the Grant No. FQXi-IAF19-06 from the Foundational Questions Institute Fund (FQXi), and a donor advised fund of the Silicon Valley Community Foundation.